sample) was almost $70 for the PCR-SSCP analysis, followed by 16S rDNA sequencing. The cost of the PCR-SSCP method can be reduced because the high reproducibility of PCR-SSCP enables the grouping of strains between different samples.

In this study, we evaluated the PCR-SSCP process as a grouping method for isolated strains from plate count analysis and showed good correlation between the PCR-SSCP analysis and 16S rDNA sequencing. Among 180 strains from various foods, 2.2% were misgrouped due to their phylogenetic relationships. This is not a substantial problem of the PCR-SSCP method because the most important aspect of this grouping method for isolates used by food suppliers is the practical usefulness. The PCR-SSCP method meets these requirements in various aspects, such as sufficient accuracy, high throughput, high reproducibility, and ease of operation. This PCR-SSCP method can also be used as the grouping method of isolates followed by identification using the identification kits and classical identification by biochemical characterization.

ACKNOWLEDGMENTS

This work was partially supported by the National Food Research Institute of Japan (project: Development of evaluation and management methods for supply of safe, reliable and functional food and farm products) and Japanese Ministry of Health, Labour and Welfare (H19-011)

REFERENCES

1. Blackwood, K. S., C. Y. Turenne, D. Harmsen, and A. M. Kabani. 2004. Reassessment of sequence-based targets for identification of *Bacillus* species. *J. Clin. Microbiol.* 42:1626–1630.
2. Brosius, J., M. L. Palmer, P. J. Kennedy, and H. F. Noller. 1978. Complete nucleotide sequence of a 16S ribosomal RNA gene from *Escherichia coli*. *Proc. Natl. Acad. Sci. USA* 75:4801–4805.
3. Chakravorty, S., D. Helb, M. Burday, N. Connell, and D. Alland. 2007. A detailed analysis of 16S ribosomal RNA gene segments for the diagnosis of pathogenic bacteria. *J. Microbiol. Methods* 69:330–339.
4. Clayton, R. A., G. Sutton, P. S. Hinkle, Jr., C. Bult, and C. Fields. 1995. Intraspecific variation in small-subunit rRNA sequences in GenBank: why single sequences may not adequately represent prokaryotic taxa. *Int. J. Syst. Bacteriol.* 45:595–599.
5. Collins, M. D., P. A. Lawson, A. Willems, J. J. Cordoba, J. Fernandez-Garayzabal, P. Garcia, J. Cai, H. Hippe, and J. A. Farrow. 1994. The phylogeny of the genus *Clostridium*: proposal of five new genera and eleven new species combinations. *Int. J. Syst. Bacteriol.* 44: 812–826.
6. De Angelis, M., R. Di Carno, G. Gallo, S. Curci, C. Siragusa, C. Crecchio, E. Parente, and M. Gobbetti. 2007. Molecular and functional characterization of *Lactobacillus sanfranciscensis*. *Int. J. Food Microbiol.* 28:69–82.
7. Don, R. H., P. T. Cox, B. J. Wainwright, K. Baker, and J. S. Mattick. 1991. "Touchdown" PCR to circumvent spurious priming during gene amplification. *Nucleic Acids Res.* 19:4008.
8. Drancourt, M., C. Bollet, A. Carta, and P. Rousselier. 2001. Phylogenetic analyses of *Klebsiella* species delineate *Klebsiella* and *Raoultella* gen. nov., with description of *Raoultella ornithinolytica* comb. nov., *Raoultella terrigena* comb. nov. and *Raoultella planticola* comb. nov. *Int. J. Syst. Evol. Microbiol.* 51:925–932.
9. Duthoit, F., J. J. Godon, and M. C. Montel. 2003. Bacterial community dynamics during production of registered designation of origin Salers cheese as evaluated by 16S rRNA gene single-strand conformation polymorphism analysis. *Appl. Environ. Microbiol.* 69: 3840–3848.
10. Ercolini, D. 2004. PCR-DGGE fingerprinting: novel strategies for detection of microbes in food. *J. Microbiol. Methods* 59:217–234.
11. Fogel, G. B., C. R. Collins, J. Li, and C. F. Brunk. 1999. Prokaryotic genome size and SSU rDNA copy number: estimation of microbial relative abundance from a mixed population. *Microb. Ecol.* 38:93–113.
12. Grahn, N., M. Hmani-Aifa, K. Fransen, P. Soderkvist, and H. J. Monstein. 2005. Molecular identification of Helicobacter DNA present in human colorectal adenocarcinomas by 16S rDNA PCR amplification and pyrosequencing analysis. *J. Med. Microbiol.* 54:1031–1035.
13. Hill, K. E., C. E. Davies, M. J. Wilson, P. Stephens, M. A. O. Lewis, V. Hall, J. Brazier, and D. W. Thomas. 2002. Heterogeneity within the gram-positive anaerobic cocci demonstrated by analysis of 16S–23S intergenic ribosomal RNA polymorphisms. *J. Med. Microbiol.* 51:949–957.
14. Hill, W. E., A. Dahlberg, R. A. Garrett, P. B. Moore, D. Schlessinger, and J. R. Warner (ed.). 1990. The ribosome: structure, function and evolution. American Society for Microbiology, Washington, D.C.
15. Lee, D. H., Y. G. Zo, and S. J. Kim. 1996. Nonradioactive method to study genetic profiles of natural bacterial communities by PCR-single-strand-conformation polymorphism. *Appl. Environ. Microbiol.* 62:3112–3120.
16. Muyzer, G., E. C. De Waal, and A. G. Uitterlinden. 1993. Profiling of complex microbial populations by denaturing gradient gel electrophoresis analysis of polymerase chain reaction-amplified genes coding for 16S rRNA. *Appl. Environ. Microbiol.* 59:695–700.
17. Mylvaganam, S., and P. P. Dennis. 1992. Sequence heterogeneity between the two genes encoding 16S rRNA from the halophilic archaebacterium *Haloarcula marismortui*. *Genetics* 130:399–410.
18. Neefs, J. M., Y. Van de Peer, L. Hendriks, and R. D. Wachter. 1990. Compilation of small ribosomal subunit RNA sequences. *Nucleic Acids Res.* 18:2237–2317.
19. Orita, M., H. Iwahana, H. Kanazawa, K. Hayashi, and T. Sekiya. 1989. Detection of polymorphisms of human DNA by gel electrophoresis as single-strand conformation polymorphisms. *Proc. Natl. Acad. Sci. USA* 86:2766–2770.
20. Peters, S., S. Koschinsky, F. Schwieger, and C. C. Tebbe. 2000. Succession of microbial communities during hot composting as detected by PCR-single-strand-conformation polymorphism-based genetic profiles of small-subunit rRNA genes. *Appl. Environ. Microbiol.* 66: 930–936.
21. Rantsiou, K., R. Urso, L. Iacumin, C. Cantoni, P. Cattaneo, G. Comi, and L. Cocolin, L. 2005. Culture-dependent and independent methods to investigate the microbial ecology of Italian fermented sausages. *Appl. Environ. Microbiol.* 71:1977–1986.
22. Schwieger, F., and C. C. Tebbe. 1998. A new approach to utilize PCR-single-strand-conformation polymorphism for 16S rRNA gene-based microbial community analysis. *Appl. Environ. Microbiol.* 64: 4870–4876.
23. Takahashi, H., B. Kimura, M. Yoshikawa, S. Gotou, I. Watanabe, and T. Fujii. 2004. Direct detection and identification of lactic acid bacteria in a food processing plant and in meat products using denaturing gradient gel electrophoresis. *J. Food Prot.* 67:2515–2520.
24. Takahashi, T., I. Satoh, and N. Kikuchi. 1999. Phylogenetic relationships of 38 taxa of the genus *Staphylococcus* based on 16S rRNA gene sequence analysis. *Int. J. Syst. Bacteriol.* 49:725–728.
25. Turenne, C. Y., E. Witwicki, D. J. Hoban, J. A. Karlowsky, and A. M. Kabani. 2000. Rapid identification of bacteria from positive blood cultures by fluorescence-based PCR-single-strand conformation polymorphism analysis of the 16S rRNA gene. *J. Clin. Microbiol.* 38:513–520.
26. Vandamme, P., J. F. Bernardet, P. Segers, K. Kersters, and B. Holmes. 1994. New perspectives in the classification of the *Flavobacteria*: description of *Chryseobacterium* gen. nov., *Bergeyella* gen. nov., and *Empedobacter* nom. rev. *Int. J. Syst. Bacteriol.* 44:827–831.
27. Weisburg, W. G., S. M. Barns, D. A. Pelletier, and D. J. Lane. 1991. 16S ribosomal DNA amplification for phylogenetic study. *J. Bacteriol.* 173:697–703.
28. Widjojoatmodjo, M. N., A. C. Fluit, and J. Verhoef. 1994. Rapid identification of bacteria by PCR-single-strand conformation polymorphism. *J. Clin. Microbiol.* 32:3002–3007.
29. Yu, Z., and M. Morrison. 2004. Comparisons of different hypervariable regions of *rrs* genes for use in fingerprinting of microbial communities by PCR-denaturing gradient gel electrophoresis. *Appl. Environ. Microbiol.* 70:4800–4806.

Available online at www.sciencedirect.com
ScienceDirect
Journal of Microbiological Methods 72 (2008) 313–320
Journal of Microbiological Methods
www.elsevier.com/locate/jmicmeth

Multiple-locus variable-number of tandem-repeats analysis distinguishes *Vibrio parahaemolyticus* pandemic O3:K6 strains

Bon Kimura [a,*], Yohko Sekine [a], Hajime Takahashi [a], Yuichiro Tanaka [a], Hiromi Obata [b], Akemi Kai [b], Satoshi Morozumi [b], Tateo Fujii [a]

[a] *Tokyo University of Marine Science and Technology, Department of Food Science and Technology, Minato Tokyo 108-8477, Japan*
[b] *Tokyo Metropolitan Institute of Public Health, Department of Microbiology, Shinjuku Tokyo 169-0073, Japan*

Received 6 November 2007; received in revised form 15 December 2007; accepted 31 December 2007
Available online 10 January 2008

Abstract

A specific serotype of *Vibrio parahaemolyticus*, O3:K6, has recently been linked to epidemics of gastroenteritis in Southeast Asia, Japan, and North America. These pandemic O3:K6 strains appear to have recently spread across continents from a single origin to reach global coverage, based on profiling of strains by several molecular typing methods. In this study, variable-number tandem repeats (VNTR)-based fingerprinting was applied to clinical and environmental *V. parahaemolyticus* O3:K6 strains in an attempt to develop a molecular method with increased sensitivity for discriminating strains; the relative discriminatory powers were compared with ribotyping and pulsed-field gel electrophoresis (PFGE). All clinical strains tested were independent human isolates obtained from different outbreaks or from sporadic cases in Tokyo during the period from 1996 to 2003. Multiple-locus VNTR analysis (MLVA) was shown to have high resolution and reproducibility for typing of *V. parahaemolyticus* clones. MLVA analysis of 28 pandemic *V. parahaemolyticus* O3:K6 strains isolated from human cases produced 28 distinct VNTR patterns. The VNTR loci displayed between 2 and 15 alleles at each of eight loci with Nei's diversity index ranging from 0.35 and 0.91. These data demonstrated that MLVA is useful for individual strain typing of new O3:K6 strains, which appear to be closely related by other molecular methods.

Keywords: DNA typing; MLVA; *Vibrio parahaemolyticus*; VNTR

1. Introduction

Vibrio parahaemolyticus is a gram-negative marine bacterium that causes seafood-borne gastroenteritis; but not all strains have the same pathogenic potential. Infections are usually caused by *V. parahaemolyticus* of diverse serotypes, and until 1996, infections were characterized by sporadic cases caused by multiple, diverse serotypes. However, recent studies have shown the emergence of serotype O3:K6, a unique serotype that is characterized by the potential to spread and to be associated with infections more often than other serotypes. In February 1996, strains belonging to the O3:K6 serotype were first documented in Calcutta, India, and accounted for 50 to 80% of the strains of *V. parahaemolyticus* responsible for infections occurring annually since then (Okuda et al., 1997). Furthermore, strains belonging to the new O3:K6 serotype have been isolated from other Southeast Asian countries, from travelers at a quarantine station in Japan (Okuda et al., 1997), and from a food-borne outbreak in the United States (Centers for Disease Control and Prevention, 1999). These isolates possessed the *tdh* gene encoding thermostable direct hemolysin (TDH), lacked the *trh* gene encoding TDH-related hemolysin, and showed very similar profiles by several molecular methods (Matsumoto et al., 2000; Nasu et al., 2000; Wong et al., 2000), suggesting the presence of a common ancestor.

* Corresponding author. Mailing address: Department of Food Science and Technology, Faculty of Marine Science, Tokyo University of Marine Science and Technology, 4-5-7 Konan, Minato, Tokyo 108-8477, Japan. Tel./fax: +81 3 5463 0603.
E-mail address: kimubo@kaiyodai.ac.jp (B. Kimura).

0167-7012/$ - see front matter © 2008 Elsevier B.V. All rights reserved.
doi:10.1016/j.mimet.2007.12.014

A variety of molecular typing methods have been applied to *V. parahaemolyticus*; ribotyping (Bag et al., 1999; DePaola et al., 2003; Gendel et al., 2001), pulsed-field gel electrophoresis (PFGE) (Bag et al., 1999; Marshall et al., 1999), group-specific PCR (GS-PCR) (Matsumoto et al., 2000), arbitrarily primed PCR (AP-PCR) (Hara-Kudo et al., 2003; Matsumoto et al., 2000; Okuda et al., 1997), and multilocus sequence typing (MLST) (Chowdhury et al., 2004). However, newly identified O3:K6 strains are shown to be genetically homogeneous, and it makes difficult to distinguish them by above methods. Therefore, we decided to develop a method that targets the short tandem repeat sequences (TRs), which undergo rapid evolution in the bacterial genome. Increasingly, variable-number tandem repeats (VNTRs) have been used to discriminate among individual strains within several food- or waterborne pathogen with little genetic variation, including *Escherichia coli* O157:H7 (Lindstedt et al., 2004a; Noller et al., 2003), *Pseudomonas aeruginosa* (Onteniente et al., 2003), *Staphylococcus aureus* (Sabat et al., 2003), *Salmonella. enterica* subsp. *enterica* serovar Typhimurium (Lindstedt et al., 2004b). Short sequence repeats, including VNTRs, consist of unique DNA elements that are repeated in tandem. Individual strains within a bacterial species often maintain the same sequence elements but with different copy numbers, variation introduced by slipped-strand mispairing during DNA replication (Metzgar et al., 2001). Since sequence homologies between strains exist in the flanking-sequences, specific primers can be used to determine the variation in copy numbers of repeat units, reflecting intraspecific genetic diversity.

The primary aim of this study was to develop a high-resolution typing system for *V. parahaemolyticus* serotype O3:K6 based on polymorphisms at genomic VNTR loci. We demonstrate the utility of this approach by comparing PFGE results for clinical strains of *V. parahaemolyticus* serotype O3:K6 from different outbreaks in Tokyo occurring from 1996 to 2003. This study shows for the first time that clonal pandemic O3:K6 strains are distinguishable by differing VNTR patterns.

2. Materials and methods

2.1. Bacterial strains

All *V. parahaemolyticus* strains ($n=34$) were collected by the Tokyo Metropolitan Institute of Public Health and provided to the Food Microbiology Laboratory at the Tokyo University of Marine Science and Technology (Table 1). Among them, 28 were clinical strains isolated from single patients associated with different outbreaks or sporadic cases in Tokyo during the period from 1996 to 2003 and the other 6 strains were environmental strains isolated from either food or seawater during the period from 1999 to 2003. All *V. parahaemolyticus* strains were grown in LB broth or on LB agar (1.5% agar) with 3% sodium chloride. All strains were serotyped by the slide agglutination test with O- and K- antigen using commercially available antisera (*V. parahaemolyticus* antisera Seiken set, Denka Seiken, Tokyo, Japan), and the presence of the *tdh* gene and *trh* gene in the isolates were determined by the primers described previously (Okura et al., 2003).

2.2. GS-PCR

GS-PCR for *toxRS* sequence of the newly emerging *V. parahaemolyticus* serotype O3:K6 clones (*toxRS/new*) and old O3:K6 strains (*toxRS/old*) was performed according to the reports by Okura et al. (2003), and ORF8 PCR for detection of the f237 filamentous phage which is unique to the newly emerged O3:K6 clones (Nasu et al., 2000) was also performed (Okura et al., 2003).

2.3. Automated ribotyping

Ribotyping was carried out using the Qualicon RiboPrinter Microbial Characterization System (Qualicon, Inc., Wilmington, Del.) according to the manufacturer's instructions. Riboprint patterns for each strain were compared to the patterns produced for all other strains using the same restriction enzyme using the software supplied with the Riboprinter system. Strain-to-strain comparisons were used to define ribogroups, each consisting of patterns that were >0.90 similar. The sample number of the first pattern in each group became the label used to identify that group. The analysis software derived a single average pattern for each ribogroup, as well as information on the similarity of each pattern within the group to the group average pattern.

2.4. Typing O3:K6 strains by PFGE

PFGE typing of strains was performed on genomic DNA digested with restriction enzyme *Not* I, as described elsewhere (Hara-Kudo et al., 2003; Yeung et al., 2002) with minor modifications. All strains were grown overnight at 30 °C in LB broth. Bacteria were harvested by centrifugation and resuspended in 100 μl resuspension buffer (Bio-Rad Laboratories Ltd., Richmond, Calif.). Agarose plugs were prepared by mixing equal volumes of bacterial suspensions. Suspensions were transferred to disposable plug molds and cooled to 4 °C. Bacterial cells in the agarose plugs were treated with lysozyme solution at 25 °C for 2 h, after which, the plugs were suspended in 300 μl of proteinase buffer containing 3 μl of proteinase K and incubated at 50 °C for overnight. Agarose plugs were washed once with wash buffer, once with 1 mM PMSF, twice with wash buffer, and once with 0.1 × wash buffer with wash time of 1 h each. Agarose plugs containing genomic DNA were digested with 10 U of *Not* I (Takara Bio Inc., Shiga, Japan) at 25 °C overnight. PFGE was performed with 1% agarose gel (Seakem Agarose Gold; FMC Bioproducts, Rockland, Me.) on a CHEF-DR II apparatus (Bio-Rad) in 0.5 × TBE buffer at 14 °C. Electrophoresis was performed at 6 V/cm for 18 h with a 2- to 40- s linear ramp time.

2.5. Searching potential VNTRs

All VNTR loci were selected using MICAS (http://www.cdfd.org.in/micas/) (Sreenu et al., 2003) and the Tandem Repeat Finder program (http://tandem.biomath.mssm.edu/trf/trf.html) (Benson, 1999) from the entire genomic sequence of *V. parahaemolyticus* RIMD2210633, Kanagawa-phenomenon positive, serotype O3:K6 (Makino et al., 2003), GenBank

Table 1
Vibrio parahaemolyticus strains used in this study

Source	Strains[a]	Serotype[b]	Year[b]	*tdh*[c]	*trh*[c]	GS-PCR *toxRS/new*[d]	GS-PCR ORF8[d]	Riboprinting DuPont ID	Riboprinting Ribogroup[e]
Clinical	V96-110	O3:K6	1996	+	−	+	+	<none>	172-48-s-3
	V96-178	O3:K6	1996	+	−	+	+	DUP-6626	172-48-s-3
	V96-223	O3:K6	1996	+	−	+	+	DUP-6626	172-48-s-3
	V97-19	O3:K6	1997	+	−	+	+	DUP-6626	172-54-s-4
	V97-49	O3:K6	1997	+	−	+	+	DUP-6626	172-48-s-3
	V97-204	O3:K6	1997	+	−	+	+	DUP-6626	172-48-s-3
	V98-10	O3:K6	1998	+	−	+	+	DUP-6626	172-48-s-1
	V98-290	O3:K6	1998	+	−	+	+	DUP-6626	172-48-s-3
	V98-324	O3:K6	1998	+	−	+	+	DUP-6626	172-48-s-3
	V99-38	O3:K6	1999	+	−	+	+	DUP-6626	172-48-s-3
	V99-107	O3:K6	1999	+	−	+	+	DUP-6626	172-48-s-3
	V99-205	O3:K6	1999	+	−	+	+	DUP-6626	172-48-s-3
	V00-76	O3:K6	2000	+	−	+	+	DUP-6626	172-48-s-3
	V00-145	O3:K6	2000	+	−	+	+	DUP-6626	172-48-s-3
	V00-161	O3:K6	2000	+	−	+	+	DUP-6626	172-48-s-3
	V01-38	O3:K6	2001	+	−	+	+	DUP-6626	172-48-s-3
	V01-141	O3:K6	2001	+	−	+	+	DUP-6626	172-48-s-3
	V01-151	O3:K6	2001	+	−	+	+	DUP-6626	172-48-s-3
	V02-21	O3:K6	2002	+	−	+	+	DUP-6626	172-48-s-1
	V02-36	O3:K6	2002	+	−	+	+	DUP-6626	172-48-s-1
	V02-64	O3:K6	2002	+	−	+	+	DUP-6626	172-48-s-3
	V02-106	O3:K6	2002	+	−	+	+	<none>	172-48-s-4
	V02-123	O3:K6	2002	+	−	+	+	DUP-6626	172-48-s-3
	V02-207	O3:K6	2002	+	−	+	+	DUP-6626	172-48-s-3
	V02-279	O3:K6	2002	+	−	+	+	DUP-6626	172-48-s-3
	V03-80	O3:K6	2003	+	−	+	+	DUP-6626	172-48-s-1
	V03-108	O3:K6	2003	+	−	+	+	DUP-6626	172-48-s-3
	V03-159	O3:K6	2003	+	−	+	+	DUP-6626	172-56-s-8
Environment	V19	O3:K6	1999	−	−	−	−	<none>	172-58-s-1
	V37	O3:K6	1999	−	−	−	−	<none>	172-58-s-2
	V71	O3:K6	1999	−	−	−	−	<none>	172-58-s-3
	V237	O3:K6	2000	−	−	−	−	<none>	172-58-s-4
	V238	O3:K6	2000	−	−	−	−	<none>	172-58-s-5
	V282	O3:K6	2003	−	−	−	−	<none>	172-58-s-5

[a] All strains were isolated in Tokyo, Japan.
[b] Year of isolation.
[c] The presence of these genes were determined by the PCR as described previously (Okura et al., 2003).
[d] Determined by the group-specific PCR for the newly emerged O3:K6 strains, performed as described previously (Okura et al., 2003).
[e] Ribogroups were designated such that identical riboprint patterns are grouped into the same ribogroup.

accession numbers BA000031 and BA000032 (Fig. 1). PCR primers were designed from sequences flanking the respective loci (Table 2).

2.6. MLVA typing

Chromosomal DNA was extracted and purified from overnight cultures by phenol-chloroform extraction and ethanol precipitation according to the method of Murray and Thompson (1980).

Primers were designed for the amplification and sequencing of the target repeat region (Table 2) to verify that the observed differences were due to variability in the tandem repeat region and not other genetic characteristics. Each 50 μl PCR mixture contained 5 μl of 10 × PCR buffer, 4 μl each deoxyribonucleotide, 5 μM of each primer, 0.25 μl of *Taq* DNA polymerase (Takara Bio Inc.), and 1 μl of DNA template. The samples were placed on a GeneAmp PCR System 9700 (Applied Biosystems, Foster City, Calif.) and the temperature was raised to 94 °C for 5 min, followed by 25 cycles of 94 °C for 30 s, 60 °C for 30 s, and 72 °C for 60 s. The final hold was for 7 min at 72 °C. All steps in the PCR thermal cycling program were identical for the 7 primer pairs, except for annealing temperatures (given in Table 2). The PCR products were then purified by polyethyleneglycol precipitation (Sambrook et al., 1989).

The forward and reverse strands of the PCR products were sequenced using an ABI PRISM 310 Genetic Analyzer (Applied Biosystems) and BigDye Terminator Cycle Sequencing kit (Applied Biosystems). Contigs were created using the base calling and fragment assembling software programs, GENETYX/ATSQ (Software Development, Tokyo, Japan) and the numbers of repeats in aligned sequences were counted. The resulting data were imported back into BioNumerics software version 4.0 (Applied-Maths, Kortrijk, Belgium) for use clustering analysis with the categorical coefficient and Ward clustering parameter. Use of the categorical coefficient implies that the character states are considered unordered. The

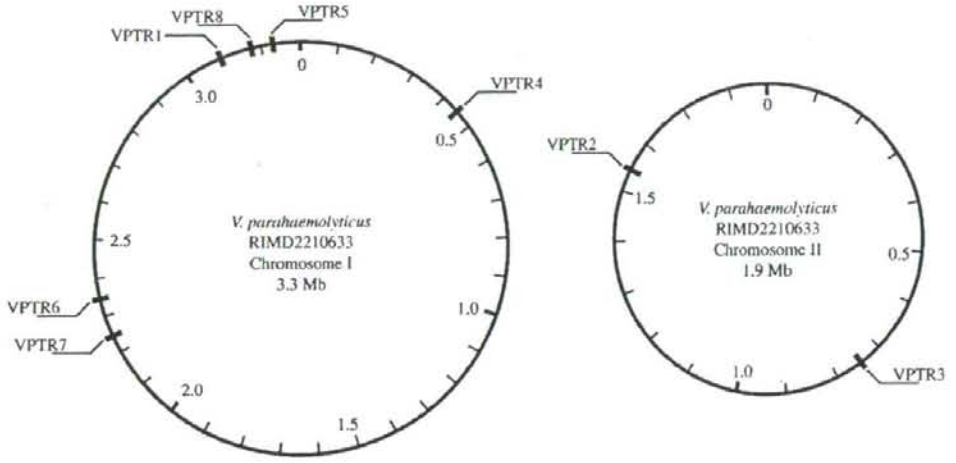

Fig. 1. VNTR maker locations within the physical map of the *V. parahaemolyticus* RIMD2210633 genome. Positions are given with reference to predicted origin of replication (set as position 0).

same weight is given to a large or a small number of differences in the number of repeats at any locus. The information index or Nei's diversity index (D) was calculated for each markers as $1-\Sigma(\text{allele frequency})^2$.

3. Results

The serotypes, virulence attributes, the results of GS-PCR for *toxRS* and ORF8, ribotyping and the sources of the 34 tested *V. parahaemolyticus* strains are shown in Table 1. PCR analysis confirmed the presence of *tdh* and the absence of *trh* in all 28 clinical strains of *V. parahaemolyticus* serotype O3:K6, while all 6 environmental strains of *V. parahaemolyticus* serotype O3:K6 lacked both *tdh* and *trh*. In addition, all 28 clinical strains were confirmed to be pandemic strains by the GS-PCR assay for *toxRS* and the ORF8 PCR assay which detects the presence of the f237 phage (Nasu et al., 2000). On the other hand, all 6 environmental strains were distinguished as nonpandemic strains by these PCR assays.

3.1. Automated ribotyping

Riboprint patterns generated for all 34 strains of *V. parahaemolyticus* O3:K6 using *Eco*RI (Table 1) showed that among the 28 clinical strains, 26 strains were identified as DuPont ID 6626 (DUP-6626; *V. parahaemolyticus*). Two

Table 2
Characteristics of the VNTR locus in *V. parahaemolyticus* and primers for MLVA

Locus	Repeat motif	Repeat times[a]	Function	Diversity[b]	Primer	Primer sequence (5′–3′)	Annealing temperature (°C)	Product size (bp)
VPTR1	ATAGAG	28	hypothetical protein	0.91	VPTR1-F	TAACAACGCAAGCTTGCAACG	60	255
					VPTR1-R	TCATTCTCGCCACATAACTCAGC		
VPTR2	CAGCAA	28	hypothetical protein	0.90	VPTR2-F	GTTACCAAACTGGCGATTACGAAG	60	615
					VPTR2-R	CGGAATTCAGGATCATCCTGAT		
VPTR3	ATCTGT	6	putative collagenase	0.35	VPTR3-F	CGCCAGTAATTCGACTCATGC	60	333
					VPTR3-R	AAGACTGTTCCCGTCGCTGA		
VPTR4	TGTGTC	7	putative hemolysin	0.43	VPTR4-F	AAACGTCTCGACATCTGGATCA	61	229
					VPTR4-R	TGTTTGGCTATGTAACCGCTCA		
VPTR5	CTCAAA	7	Non-coding region	0.56	VPTR5-F	GCTGGATTGCTGCGAGTAAGA	60	202
					VPTR5-R	AACTCAAGGGCTGCTTCGG		
VPTR6	GCTCTG	17	hypothetical protein	0.79	VPTR6-F	TGTCGATGGTGTTCTGTTCCA	60	312
					VPTR6-R	CTTGACTTGCTCGCTCAGGAG		
VPTR7	CTGCTC	6	hypothetical protein	0.38	VPTR7-F	CAACAGTTCTGCTCTAATCTTCCG	56	221
					VPTR7-R	CAAAGGTGTTACTTGTTCCAGACG		
VPTR8	CTTCTG	7	Cell division protein	0.44	VPTR8-F	ACATCGGCAATGAGCAGTTG	60	306
					VPTR8-R	AAGAGGTTGCTGAGCAAGCG		

[a] Numbers of tandem repeats were counted using the genome sequence of *V. parahaemolyticus* RIMD2210633 (Makino et al., 2003).
[b] Diversity is based on Nei's marker diversity, which is $1-\Sigma(\text{allele frequency})^2$.

strains not identified as DUP-6626, V96-110 and V02-106, showed similarities with DUP-6626 of 84% and 74%, respectively (Table 1). The majority (22 strains) of the 28 clinical strains were grouped in ribogroup 172-48-s-3 (average internal similarity, 95.9%), and 4 strains in ribogroup 172-48-s-1 had an average internal similarity 97.5%. Ribogroup 172-48-s-3 has similarity of 93%, and 172-48-s-1, 91%, with DUP-6626. All the environmental strains had no DuPont ID (Table 1).

3.2. PFGE profiles

In this study, PFGE was carried out with *Not* I. Previous experiments indicated that pandemic O3:K6 clones show similar PFGE patterns (Arakawa et al., 1999; Chowdhury et al., 2000; Yeung et al., 2002). In this study, obvious distinction between clinical and environmental strains was noted (Fig. 2). Furthermore, clinical O3:K6 group strains had highly similar PFGE patterns; all pandemic strains tested in this study displayed PFGE pattern A, except for the isolates V00-76, V00-145, V00-161, V02-21 and V02-36, which were internally identical and showed small one-band differences from the pattern A PFGE profile (PFGE pattern B). Three strains, V01-141, V01-151, and V02-207, were untypeable producing only a smear of bands on the gels. This is in accordance with previous studies (Marshall et al., 1999; Yeung et al., 2002) and suggests that the utility of PFGE for differentiating *V. parahaemolyticus*

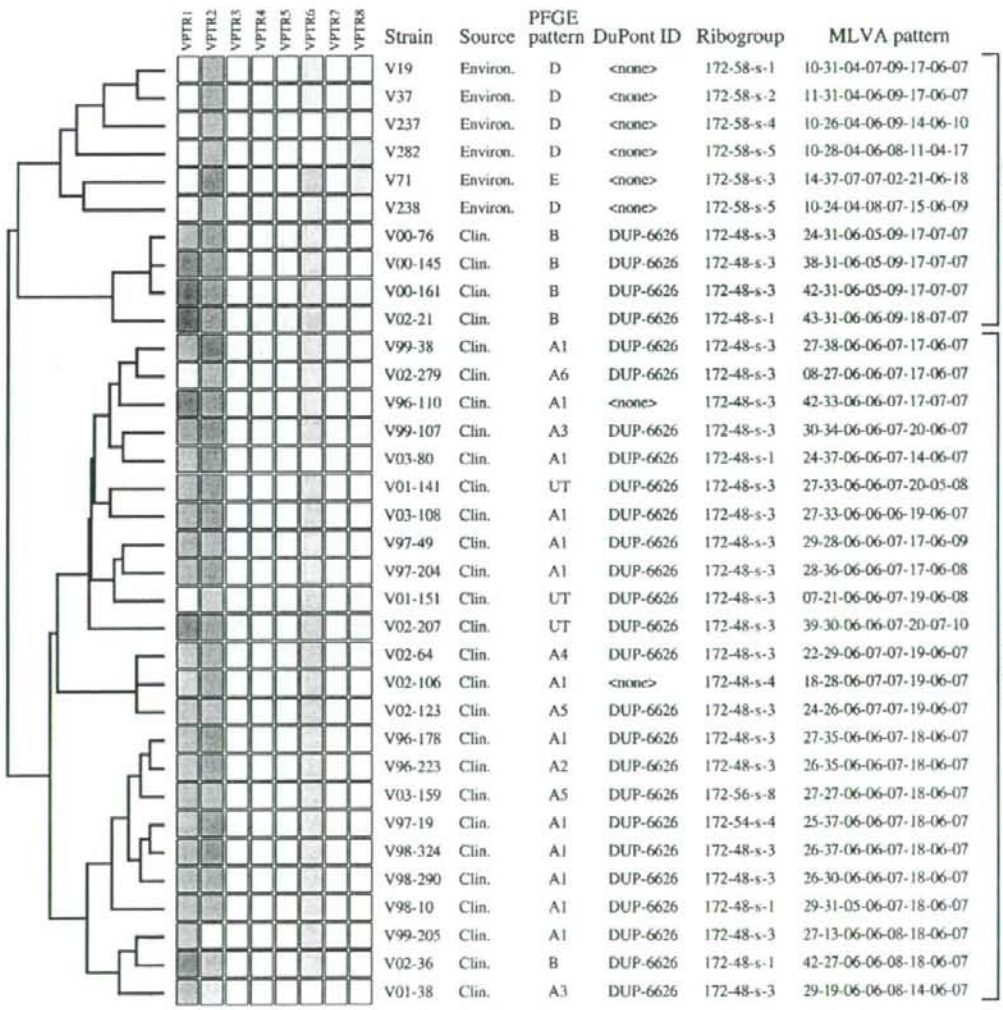

Fig. 2. The dendrogram of all the MLVA-typed *V. parahaemolyticus* O3:K6 strains. The frequencies of tandem repeats of each locus were visualized by the grayscale matrices (the color density indicates the frequency of each tandem repeats). The PFGE profile and DuPont ID generated from ribotyping are also shown. Ribogroups were designated such that identical riboprint patterns were grouped into the same ribogroup. Abbreviations: <none>, No corresponded DuPont ID; UT, untypeable.

Table 3
The number of tandem repeats of the *V. parahaemolyticus* strains used in this study

		Repeat times (Repeat motif)							
		VPTR1	VPTR2	VPTR3	VPTR4	VPTR5	VPTR6	VPTR7	VPTR8
Source	Strains	(ATAGAG)	(CAGCAA)	(ATCTGT)	(TGTGTC)	(CTCAAA)	(GCTCTG)	(CTGCTC)	(CTTCTG)
Clinical	V96-110	42	33	6	6	7	17	7	7
	V96-178	27	35	6	6	7	18	6	7
	V96-223	26	35	6	6	7	18	6	7
	V97-19	25	37	6	6	7	18	6	7
	V97-49	29	28	6	6	7	17	6	9
	V97-204	28	36	6	6	7	17	6	8
	V98-10	29	31	5	6	7	18	6	7
	V98-290	26	30	6	6	7	18	6	7
	V98-324	26	37	6	6	7	18	6	7
	V99-38	27	38	6	6	7	17	6	7
	V99-107	30	34	6	6	7	20	6	7
	V99-205	27	13	6	6	8	18	6	7
	V00-76	24	31	6	5	9	17	7	7
	V00-145	38	31	6	5	9	17	7	7
	V00-161	42	31	6	5	9	17	7	7
	V01-38	29	19	6	6	8	14	6	7
	V01-141	27	33	6	6	7	20	5	8
	V01-151	7	21	6	6	7	19	6	8
	V02-21	43	31	6	6	9	18	7	7
	V02-36	42	27	6	6	8	18	6	7
	V02-64	18	29	6	7	7	19	6	7
	V02-106	18	28	6	7	7	19	6	7
	V02-123	24	26	6	7	7	19	6	7
	V02-207	39	30	6	6	7	20	7	10
	V02-279	8	27	6	6	7	17	6	7
	V03-80	24	37	6	6	7	14	6	7
	V03-108	27	33	6	6	6	19	6	7
	V03-159	27	27	6	6	7	18	6	7
Environment	V19	10	31	4	7	9	17	6	7
	V37	11	31	4	6	9	17	6	7
	V71	14	37	7	7	2	21	6	18
	V237	10	26	4	6	9	14	6	10
	V238	10	24	4	8	7	15	6	9
	V282	10	28	4	6	8	11	4	17

might be limited by some of isolates untypeable due to DNA degradation.

3.3. PCR amplification and sequence analysis of potential VNTRs

A total of eight VNTR loci were analyzed in the *V. parahaemolyticus* genome, which consists of two circular chromosomes; six VNTRs were localized on chromosome I, and two were localized on chromosome II (Fig. 1). All eight VNTR loci were successfully amplified, and sufficient variability was confirmed in the eight VNTR loci by sequencing. We found that all eight loci had multiple alleles with substantial variability. In all cases, the size variation observed among PCR products was attributable to the number of TRs.

The VNTRs loci displayed a wide range of polymorphisms in the O3:K6 strains, with the VPTR1 and VPTR2 being the most polymorphic (Table 3). Among 28 clinical strains, VPTR1 had 18 different alleles, and VPTR2 had 16, VPTR6 had 5, VPTR5 and VPTR8 each had 4, VPTR4 and VPTR7 each had 3, and VPTR3 had only 2. The Nei's diversity index (D) is based on the number of alleles and the allele frequency and provides a better measure of discriminatory power than allele number; D values for VNTR markers in this study ranged from 0.35 for VPTR3 to 0.91 for VPTR1. VNTR analysis showed a high degree of discrimination of the O3:K6 strains.

3.4. MLVA dendrogram

The extent of genetic diversity among the tested strains based on the MLVA dendrogram revealed that each strain has a distinct profile; that is, 34 strains produced 34 patterns (Fig. 2). Only minor discrepancies were noted between the cluster pattern profiles generated by MVLA and the PFGE (Fig. 2). In MLVA analysis, two main groups, denoted as groups I and II, each were comprised of smaller groups or individual isolates. Cluster I contained all environmental O3:K6 strains and 6 pandemic O3:K6 strains. Cluster II contained the remaining pandemic O3:K6 strains. Closer inspection of cluster I, however, revealed that the pandemic O3:K6 isolates in this

cluster (V00-76, V00-145, V00-161, V02-21) in MLVA had distinct,one-band differences from the major group of the pandemic O3:K6 strains identified by PFGE (data not shown). On the other hand, the majority of strains that clustered together in PFGE produced distinct VNTR profiles, suggesting that distinct populations of *V. parahaemolyticus* serotype O3:K6 strains may have circulated during sporadic cases or in outbreaks in Tokyo during the period from 1996 to 2003. The lack of multiple isolates from the same outbreak did, however, prevent a through analysis of isolate populations.

4. Discussion

The main finding of this study was the high discrimination power of MLVA for the pandemic serotype O3:K6 strains of *V. parahaemolyticus*. All 28 of pandemic serotype O3:K6 strains tested here could be discriminated as individual strains (28 different MLVA profiles, Fig. 2). This is important since no other available typing method provides high-resolution discrimination among pandemic serotype O3:K6 strains. Previous studies using molecular analysis of O3:K6 isolates collected recently from several countries had suggested the genetic homogeneity of O3:K6 (Arakawa et al., 1999; Chowdhury et al., 2000; Matsumoto et al., 2000). The genetic homogeneity of these newly isolated O3:K6 strains were also confirmed by GS-PCR, ribotyping, and PFGE in this study. Although the clinical strains used in this study were isolated from different outbreaks or from sporadic cases during period from 1996 to 2003 in Tokyo, almost all were shown to be identical by these methods (Table 1, Fig. 2), supporting the view of previous studies that pandemic strains might have originated from the same clone (Chowdhury et al., 2000; Okuda et al., 1997). However, our MLVA results showed a high resolution for these pandemic strains, indicating substantial genetic heterogeneity at the VNTR loci among pandemic *V. parahaemolyticus* O3:K6 strains. The finding of great diversity within the small set of *V. parahaemolyticus* O3:K6 strains studied here suggests that there is still a great deal of unsampled *V. parahaemolyticus* O3:K6 diversity to be discovered. One potential concern is that VNTRs evolve so rapidly that multiple MLVA types emerge during outbreak or cultural transfers. A number of studies, however, have revealed that the composition of the VNTR loci is relatively stable and does not change even after prolonged storage or subculture in laboratory settings (Adair et al., 2000; Keim et al., 2000; Sabat et al., 2003; Truman et al., 2004). In this study, we have not tested the stability and heterogeneity within the bacterial population after extensive subculturing of individual colonies of *V. parahaemolyticus*. Thus, further studies on cultural stability and larger collections from various origins including outbreak strains are necessary to validate the application of VNTRs for the characterization of *V. parahaemolyticus*.

The functions of VNTRs used for MLVA typing in this study remain unknown, and the relationships between VNTRs and potential mechanisms for metabolic regulation as well as antigenic variation and environmental adaptation should be further examined. The VNTR loci analyzed here are widely distributed across chromosome I and II of RIMD2210633 (Fig. 1). With the exception of VPTR5, which is located in a non-coding region, VNTRs analyzed here are all located in open reading frame regions. The repeat units in the VNTRs studied in this study were all 3-bp multiples, indicating that variation in the number of repeats in these genes results in altered amino acid sequence, but not in inactivation of genes due to frame shifting. VPTR1, VPTR2, VPTR6, and VPTR7 are located in open reading frames that hypothetically codes for proteins. Allele states of the VPTR1 and VPTR2 loci are highly variable, having 18 and 16 alleles respectively. VPTR3 is located in an open reading frame that codes for the putative collagenase gene. Collagenase digests collagen, affecting the basic structure of membranes in eucaryotic cells. Studies in *V. parahaemolyticus* and *V. cholerae* have shown that collagenase activity may play a role on the virulence and be a factor in host infection and pathogenesis. Apparently, variation in VPTR3 for this gene is limited, and clinical strains, except for V98-10, have 6 repeats, indicating the essential role of putative collagenase gene in the bacterial cell. VPTR4 is located in an open reading frame that codes for the putative hemolysin gene. Pathogenicity of *V. parahaemolyticus* has been correlated to well-characterized hemolysin, TDH and TRH (Honda and Iida, 1993; Naim et al., 2001). Thermolabile direct hemolysin (TLH) (Taniguchi et al., 1990) and lectin-dependent hemolysin (LDH) (Shinoda et al., 1991) have also been reported as the virulence factors of this bacterium. However, the putative hemolysin gene which includes VPTR4 is apparently different from the above hemolysin genes. Since both clinical and environmental strains of *V. parahaemolyticus* have this gene with variation in VPTR4, these genes do not to seem to be key to the virulence of this organism. Examination of the observed allelic differences of these genes among pandemic strains and the relationship to virulence or physiological differences will be interesting for future studies.

In this study, we have shown that MLVA is a valuable typing technique for characterizing recently emerged and highly homogeneous pandemic strains of *V. parahaemolyticus* serotype O3:K6. The data presented here demonstrate the utility of this approach for individual strain identification. Although MLVA loci in pandemic O3:K6 strains seem to mutate too rapidly to be useful in determining global phylogenetic relationships, they are useful for strain identification and may identify rapidly evolving polymorphisms that are useful for discriminating very closely related strains, such as *V. parahaemolyticus* serotype O3:K6 strains. In addition to high resolution power, MLVA is a simple and rapid method, which can be used to produce strain profiles that are easily exchanged electronically via the BioNumerics database as character strings. In this study, we sequenced VPTR1 to VPTR8 amplicons to verify PCR specificity and to confirm that any observed length polymorphisms were due solely to variation in VNTR copy number. However, for practical purposes, sequencing will not be necessary and this method can be further improved by using primers tagged with multiple fluorescent dyes, allowing accurate sizing of amplicons by automated DNA sequencer analysis. This method therefore gives fast, discriminative, and reproducible results for epidemiological surveillance of *V. parahaemolyticus* pandemic strains.

Acknowledgements

This work was partly supported by the National Food Research Institute of Japan (project: Development of evaluation and management methods for supply of safe, reliable and functional food and farm produce) and Japanese Ministry of Health, Labour and Welfare (H19-011).

The authors thank for Tatsuya Ishikawa for MLVA data analyses.

References

Adair, D.M., Worsham, P.L., Hill, K.K., Klevytska, A.M., Jackson, P.J., Friedlander, A.M., Keim, P., 2000. Diversity in a variable-number tandem repeat from *Yersinia pestis*. J. Clin. Microbiol. 38, 1516–1519.

Arakawa, E., Murase, T., Shimada, T., Okitsu, T., Yamai, S., Watanabe, H., 1999. Emergence and prevalence of a novel *Vibrio parahaemolyticus* O3:K6 clone in Japan. Jpn. J. Infect. Dis. 52, 246–247.

Bag, P.K., Nandi, S., Bhadra, R.K., Ramamurthy, T., Bhattacharya, S.K., Nishibuchi, M., Hamabata, T., Yamasaki, S., Takeda, Y., Nair, G.B., 1999. Clonal diversity among recently emerged strains of *Vibrio parahaemolyticus* O3:K6 associated with pandemic spread. J. Clin. Microbiol. 37, 2354–2357.

Benson, G., 1999. Tandem repeats finder: a program to analysis DNA sequences. Nucleic Acids Res. 27, 573–580.

Centers for Disease Control and Prevention, 1999. Outbreak of *Vibrio parahaemolyticus* infection associated with eating raw oysters and clams harvested from Long Island Sound — Connecticut, New Jersey, and New York, 1998. Morbid. Mortal. Weekly Rep. 48, 48–51.

Chowdhury, N.R., Stine, O.C., Morris, J.G., Nair, G.B., 2004. Assessment of evolution of pandemic *Vibrio parahaemolyticus* by multilocus sequence typing. J. Clin. Microbiol. 42, 1280–1282.

Chowdhury, N.R., Chakraborty, S., Ramamurthy, T., Nishibuchi, M., Yamasaki, S., Takeda, Y., Nair, G.B., 2000. Molecular evidence of clonal *Vibrio parahaemolyticus* pandemic strains. Emerg. Infect. Dis. 6, 631–636.

DePaola, A., Ulaszek, J., Kaysner, C.A., Tenge, B.J., Nordstrom, J.L., Wells, J., Puhr, N., Gendel, S.M., 2003. Molecular, serological, and virulence characteristics of *Vibrio parahaemolyticus* isolated from environmental, food, and clinical sources in North America and Asia. Appl. Environ. Microbiol. 69, 3999–4005.

Gendel, S.M., Ulaszek, J., Nishibuchi, M., DePaola, A., 2001. Automated ribotyping differentiates *Vibrio parahaemolyticus* O3:K6 strains associated with a Texas outbreak from other clinical strains. J. Food Prot. 64, 1617–1620.

Hara-Kudo, Y., Sugiyama, K., Nishibuchi, M., Chowdhury, A., Yatsuyanagi, J., Ohtomo, Y., Saito, A., Nagano, H., Nishina, T., Nakagawa, H., Konuma, H., Miyahara, M., Kumagai, S., 2003. Prevalence of pandemic thermostable direct hemolysin-producing *Vibrio parahaemolyticus* O3:K6 in seafood and the coastal environment in Japan. Appl. Environ. Microbiol. 69, 3883–3891.

Honda, T., Iida, T., 1993. The pathogenicity of *Vibrio parahaemolyticus* and the role of the thermostable direct hemolysin and related hemolysins. Rev. Med. Microbiol. 4, 106–113.

Keim, P., Price, L.B., Klevytska, A.M., Smith, K.L., Schupp, J.M., Okinaka, R., Jackson, P.J., Hugh-Jones, M.E., 2000. Multiple-locus variable-number tandem repeat analysis reveals genetic relationships within *Bacillus anthracis*. J. Bacteriol. 182, 2928–2936.

Lindstedt, B.A., Vardund, T., Kapperud, G., 2004a. Multiple-locus variable-number tandem-repeat analysis of *Escherichia coli* O157 using PCR multiplexing and multi-colored capillary electrophoresis. J. Microbiol. Methods 58, 213–222.

Lindstedt, B.A., Vardund, T., Aas, L., Kapperud, G., 2004b. Multiple-locus variable-number tandem-repeats analysis of *Salmonella enterica* subsp. *enterica* serovar Typhimurium using PCR multiplexing and multicolor capillary electrophoresis. J. Microbiol. Methods 59, 163–172.

Makino, K., Oshima, K., Kurokawa, K., Yokoyama, K., Uda, T., Tagomori, K., Iijima, Y., Najima, M., Nakano, M., Yamashita, A., Kubota, Y., Kimura, S., Yasunaga, T., Honda, T., Shinagawa, H., Hattori, M., Iida, T., 2003. Genomic sequence of *Vibrio parahaemolyticus*: a pathogenic mechanism distinct from that of *V. cholerae*. Lancet 361, 743–749.

Marshall, S., Clark, C.G., Wang, G., Mulvey, M., Kelly, M.T., Johnson, W.M., 1999. Comparison of molecular methods for typing *Vibrio parahaemolyticus*. J. Clin. Microbiol. 37, 2473–2478.

Matsumoto, C., Okuda, J., Ishibashi, M., Iwanaga, M., Garg, P., Rammamurthy, T., Wong, H., DePaola, A., Kim, Y.B., Albert, M.J., Nishibuchi, M., 2000. Pandemic spread of an O3:K6 clone of *Vibrio parahaemolyticus* and emergence of related strains evidenced by arbitrarily primed PCR and *toxRS* sequence analyses. J. Clin. Microbiol. 38, 578–585.

Metzgar, D., Thomas, E., Davis, C., Field, D., Wills, C., 2001. The microsatellites of *Escherichia coli*: rapidly evolving repetitive DNAs in a non-pathogenic prokaryote. Mol. Microbiol. 39, 183–190.

Murray, M., G., Thompson, W.F., 1980. Rapid isolation of high molecular weight plant DNA. Nucl. Acids Res. 8, 4321–4325.

Naim, R., Yanagihara, I., Iida, T., Honda, T., 2001. *Vibrio parahaemolyticus* thermostable direct hemolysin can induce an apoptotic cell death in Rat-1 cells from inside and outside of the cells. FEMS Microbiol. Lett. 195, 237–244.

Nasu, H., Iida, T., Sugahara, T., Yamaichi, Y., Park, K., Yokoyama, K., Makino, K., Shinagawa, H., Honda, T., 2000. A filamentous phage associated with recent pandemic *Vibrio parahaemolyticus* O3:K6 strains. J. Clin. Microbiol. 38, 2156–2161.

Noller, A.C., McEllistrem, M.C., Pacheco, A.G.F., Boxrud, D.J., Harrison, L.H., 2003. Multilocus variable-number tandem repeat analysis distinguishes outbreak and sporadic *Escherichia coli* O157:H7 isolates. J. Clin. Microbiol. 41, 5389–5397.

Okuda, J., Ishibashi, M., Hayakawa, E., Nishino, T., Takeda, Y., Mukhopadhyay, A.K., Garg, S., Bhattacharya, S.K., Nair, G.B., Nishibuchi, M., 1997. Emergence of a unique O3:K6 clone of *Vibrio parahaemolyticus* in Calcutta, India, and isolation of strains from the same clonal group from Southeast Asian travelers arriving in Japan. J. Clin. Microbiol. 35, 3150–3155.

Okura, M., Osawa, R., Iguchi, A., Arakawa, E., Terajima, J., Watanabe, H., 2003. Genotypic analyses of *Vibrio parahaemolyticus* and development of a pandemic group-specific multiplex PCR assay. J. Clin. Microbiol. 41, 4676–4682.

Onteniente, L., Brisse, S., Tassios, P.T., Vergnaud, G., 2003. Evaluation of polymorphisms associated with tandem repeats for *Pseudomonas aeruginosa* strain typing. J. Clin. Microbiol. 41, 4991–4997.

Sabat, A., Krzyszton-Russjan, J., Strzalka, W., Filipek, R., Kosowska, K., Hryniewicz, W., Travis, J., Potempal, J., 2003. New method for typing *Staphylococcus aureus* strains: multiple-locus variable-number tandem repeat analysis of polymorphism and genetic relationships of clinical isolates. J. Clin. Microbiol. 41, 1801–1804.

Sambrook, J.E., Fritsch, F., Maniatis, T.S., 1989. Molecular cloning: A Laboratory Manual, 2nd edn. Cold Spring Harbor Laboratory, Cold Spring Harbor, New York.

Shinoda, S., Matsuoka, H., Tsuchie, T., Miyoshi, S., Yamamoto, S., Taniguchi, H., Mizuguchi, Y., 1991. Purification and characterization of a lecithin-dependent hemolysin from *Escherichia coli* transformed by a *Vibrio parahaemolyticus* gene. J. Gen. Microbiol. 137, 2705–2711.

Sreenu, V.A., Alevoor, V., Nagaraju, J., Nagarajaram, H.A., 2003. MICdb: database of prokaryotic microsatellites. Nucleic Acids Res. 31, 106–108.

Taniguchi, H., Kubomura, S., Hirano, H., Mizue, K., Ogawa, M., Mizuguchi, Y., 1990. Cloning and characterization of a gene encoding a new thermostable hemolysin from *Vibrio parahaemolyticus*. FEMS Microbiol. Lett. 67, 339–345.

Truman, R., Fontes, A.B., de Miranda, A.B., Suffys, P., Gillis, T., 2004. Genotypic variation and stability of for variable-number tandem repeats and their suitability for discriminating strains of *Mycobacterium leprae*. J. Clin. Microbiol. 42, 2558–2565.

Wong, H.C., Liu, S.H., Wang, T.K., Lee, C.L., Chiou, C.S., Liu, D.P., Nishibuchi, M., Lee, B.K., 2000. Characteristics of Vibrio parahaemolyticus O3:K6 from Asia. Appl. Environ. Microbiol. 66, 3981–3986.

Yeung, P.S.M., Hayes, M.C., DePaola, A., Kaysner, C.A., Kornstein, L., Boor, K.J., 2002. Comparative phenotypic, molecular, and virulence characterization of *Vibrio parahaemolyticus* O3:K6 isolates. Appl. Environ. Microbiol. 68, 2901–2909.

Journal of Applied Microbiology ISSN 1364-5072

ORIGINAL ARTICLE

Induction of the histidine decarboxylase genes of *Photobacterium damselae* subsp. *damselae* (formally *P. histaminum*) at low pH

B. Kimura, H. Takahashi, S. Hokimoto, Y. Tanaka and T. Fujii

Department of Food Science and Technology, Faculty of Marine Science, Tokyo University of Marine Science and Technology, Tokyo, Japan

Keywords
acid induction, histidine decarboxylase, histamine, transcriptional analysis.

Correspondence
Bon Kimura, Department of Food Science and Technology, Faculty of Marine Science, Tokyo University of Marine Science and Technology, 4-5-7 Konan, Minato, Tokyo 108-8477, Japan. E-mail: kimubo@kaiyodai.ac.jp

2008/1288: Received 25 July 2008, revised 16 December 2008 and accepted 18 December 2008

doi:10.1111/j.1365-2672.2009.04223.x

Aims: To elucidate the detailed mechanism of histamine production by *Photobacterium damselae* subsp. *damselae*.

Methods and Results: Histidine decarboxylase and related genes of *P. damselae* subsp. *damselae* were cloned, and three open reading frames named as *hdcT*, *hdcA* and *hisRS* were identified. The *hdcA* gene encodes a polypeptide of 377 amino acids and is considered to be the pyridoxal-P dependent histidine decarboxylase. The *hdcT* gene is assumed to be a histidine/histamine antiporter, and the *hisRS* gene is considered to be a histidyl-tRNA synthetase. Recombinant *Escherichia coli* strains harbouring plasmids carrying the *P. damselae hdc* genes were shown to over-excrete histamine extracellularly. Northern blot analysis and quantitative RT-PCR revealed high levels of mono- and bi-cistronic transcripts of *hdcA*, *hdcT* and *hisRS* genes under conditions of low pH and histidine excess.

Conclusions: The *hdcA* gene of *P. damselae* was constructed as an operon with putative histidine/histamine antiporter and histidyl-tRNA synthetase. Mono- and poly-cistronic transcripts and acid induction were detected.

Significance and Impact of the Study: This is the first report of cloning the histidine decarboxylase gene cluster in Gram-negative bacteria. Also, these genes were induced under acidic conditions and in the presence of excess histidine.

Introduction

Histidine decarboxylase catalyses the decarboxylation of histidine to histamine and CO_2. Histamine is well known for its vasoactive properties and, along with other biogenic amines produced by bacteria in several foods, is a consumer health threat. In general, bacterial amino acid decarboxylases, such as lysine decarboxylase (Park *et al.* 1996; Merrell and Camilli 1999, 2000), arginine decarboxylase (Castanie-Cornet *et al.* 1999) and glutamate decarboxylase (Lin *et al.* 1996) are greatly induced under acidic conditions and are hypothesized to play a role in controlling pH as a countermeasure to acidity resulting from anaerobic fermentation. One of these enzymes, lysine decarboxylase (Cad A) of *Escherichia coli*, has been well characterized (Meng and Bennett 1992a,b; Watson *et al.* 1992). CadA decarboxylates intracellular lysine to cadaverine, consumes a proton, and then, cadaverine is transported extracellularly via a lysine-cadaverine antiporter (CadB). These processes provide a clear survival advantage under acidic conditions. Similar mechanisms have been proposed for other decarboxylase systems, such as glutamate decarboxylase (Waterman and Small 1996; Sanders *et al.* 1998; Castanie-Cornet *et al.* 1999; Cotter *et al.* 2001) and arginine decarboxylase (Lin *et al.* 1996), and it is now clear that these amino acid decarboxylase systems play an important role in the survival of bacteria under acidic conditions (Bearson *et al.* 1997; Merrell and Camilli 2002).

The known bacterial histidine decarboxylases fall into two groups: those that contain pyridoxal-P as the essential coenzyme and those that contain a covalently bound pyruvoyl residue at the active site. While histidine decarboxylases from Gram-positive bacteria are

pyruvoyl-dependent enzymes, those from Gram-negative bacteria are pyridoxyal-P-dependent enzymes. The amino acid sequence of pyridoxal 5′-phosphate dependent histidine decarboxylase has been studied in four bacterial species: *Morganella morgani* (Vaaler *et al.* 1986), *Raoultella planticola* (formally named *Klebsiela*), *Enterobacter aerogenes* (Kamath *et al.* 1991) and *Photobacterium phosphoreum* (Morii *et al.* 2006). However, transcriptional analysis of these enzymes under acidic conditions has not yet been carried out.

In surveys of histamine-producing bacteria in marine fish and seawater, we isolated several strains of facultatively anaerobic, halophilic bacteria that produced histamine to as large an extent as *M. morganii*. This bacterium was renamed to a new species as *P. histaminum* (Okuzumi *et al.* 1994). Recently, this species has been proposed to be a subjective synonym of *P. damselae* subsp. *damselae*, an opportunistic pathogen of fish and mammals (Kimura *et al.* 2000; Yamane *et al.* 2004). A study on the effect of culture conditions of L-histidine decarboxylation activity of this bacterium showed that decarboxylation was highest in acidic conditions (Kurihara *et al.* 1993). These analyses suggest that expression of the gene encoding histidine decarboxylase in this bacterium is controlled by acidity in the environment.

In the study reported here, we cloned and performed transcriptional analysis of the *hdc* gene cluster, which encodes histidine decarboxylase and the related genes of *P. damselae* subsp. *damselae* ATCC51805. This is the first report of the full sequence of the *hdc* gene cluster and the first transcriptional analysis of the *hdc* gene cluster for Gram-negative bacteria.

Materials and methods

Strains and media

The strain *P. damselae* ATCC 51805 used in this study was originally isolated from fish and first named as *P. histaminum* (Okuzumi *et al.* 1994) and recently reclassified as *P. damselae* subsp. *damselae* (Kimura *et al.* 2000). Half-strength artificial seawater (ASW)-PMGY broth was described previously (Okuzumi *et al.* 1981). PY broth contained 10 g of bacto peptone, 3 g of bacto yeast extract in 50% ASW and histidine broth (HB) contained 10 g of bacto peptone, 3 g of bacto yeast extract and 5 g of L-histidine per liter in 50% ASW (Okuzumi *et al.* 1981). PY-7·5 and HB-7·5 media were prepared as PY or HB buffered at pH 7·5 with a final concentration of 100 mmol l^{-1} 3-(*N*-morpholino) propanesulfonic acid (MOPS), and PY-4·5 and HB-4·5 were PY or HB buffered at pH 4·5 with a final concentration of 100 mmol l^{-1} 2-(*N*-morpholino) ethane sulfonic acid (MES).

Escherichia coli JMI09 (Yanisch-Perron *et al.* 1985) was used as host cells for the cloning and sequencing procedures and *E. coli* BL21 (DE3) was used as host cells for expression of the *hdcA* and *hdcB* genes. Luria–Bertani medium (LB, 1% tryptone, 0·5% yeast extract, and 1% NaCl) was used as a complex medium for *E. coli*. Cultures of *E. coli* were incubated aerobically at 37°C and *P. damselae* was incubated at 30°C. The plasmid pUC18 was used for cloning, and plasmids pUC18 or pUC19 (Takara Bio, Shiga, Japan) were used for expression of the cloned *hdc* genes. When required, ampicillin (50 μg ml^{-1}) was added to the culture media.

Analysis of N-terminal amino acid sequence

Cells from a 5l culture of *P. damselae* ATCC 51805 in half-strength ASW-PMGY broth were harvested in early stationary phase by centrifugation (4000 *g*, 5 min), and resuspended in buffer A (50 mmol l^{-1} KH_2PO_4, 50 mmol l^{-1} succinic acid, 2 mmol l^{-1} EDTA, 1 mmol l^{-1} DTT, 10 μmol l^{-1} PLP, pH 6·0) (Vaaler *et al.* 1986). After cells were disrupted at 4°C by ultrasonication, the supernatant was purified through ammonium sulfate precipitation and several chromatographic separations; DEAE cellulofine A-550 (Seikagaku Corporation, Tokyo, Japan), Phenyl Sepharose CL-4B (Amersham Biosciences Corp., Piscataway, NJ, USA), and Amicon ultrafiltration cell (Millipore Corp., Bedford, MA, USA). The dialysed preparation of the semi-purified effluent was applied to an anion exchange column (DEAE), gel filtrated and applied to reversed phase chromatography using HPLC. The N-terminal amino acid sequence of purified protein was determined by automated Edman degradation using a Beckman LF3000 protein sequencer (Beckman Coulter, Fullerton, CA, USA).

Cloning of the *hdc* genes and sequence analysis

Chromosomal DNA of *P. damselae* was purified by standard methods (Murray and Thompson 1980). Southern blot hybridization analysis (Sambrook *et al.* 1989) was performed using DNA probes prepared using primers 5′-GAY GCN TTY TGG GCN CAY TGY G-3′ (designed from the N-terminal amino acid sequence, DAFWAHCV) and 5′-GAR CCR ATC ATT TTG TGK CCG C-3′ (designed from known *hdcA* sequences). Based on Southern blot analysis, the restriction enzyme digests including 4·5kb fragment of *SacI–SalI* was cloned into pUC18 plasmid using DNA ligation kit (Takara Bio) and transformed into *E. coli* JM109 competent cell (Toyobo, Tokyo, Japan). Then, based on the sequence data of the cloned 4·5-kb *SacI–SalI* fragment, the adjacent two fragments were cloned based on Southern blot hybridization: 4·5kb

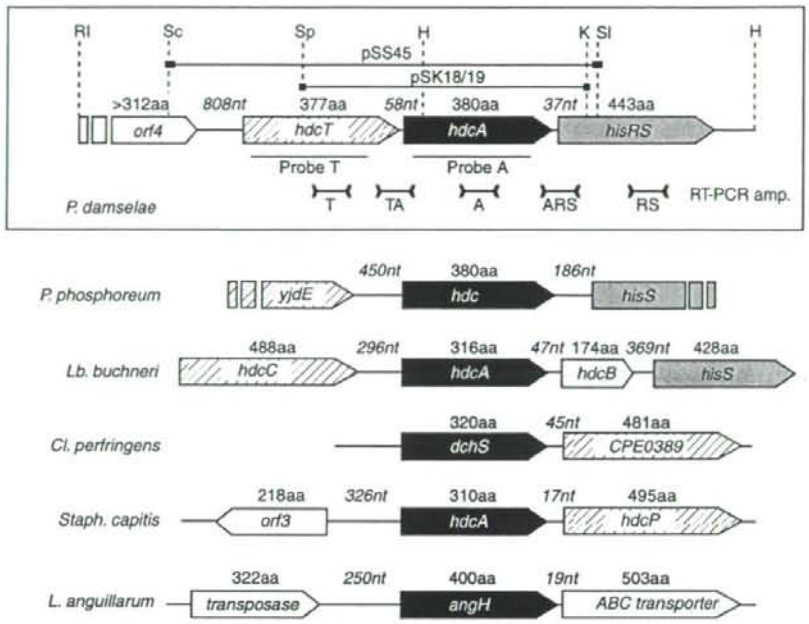

Figure 1 Schematic representation of the histidine decarboxylase gene clusters of *P. damselae* (in the box), *P. phosphoreum* (5′ and 3′ incomplete) (AY223843), *Lactobacillus buchneri* (AJ749838), *Clostridium perfringens* (BA000016), *Staphylococcus capitis* (AM283479) and *Listonella anguillarum* (AY312585). The restriction enzymes used in this report are indicated above of the *P. damselae* schematic with dashed lines. The regions targeted by DNA probes for Northern blot hybridization analysis are indicated by lines labelled with probe T or probe A, and amplification target sites for real-time PCR are indicated by the double-arrowed lines as follows: T, *hdcT* mRNA; TA, *hdcT-hdcA* bi-cistronic mRNA; A, *hdcA* mRNA; ARS, *hdcA-hisRS* bi-cistronic mRNA; and RS, *hisRS* mRNA. Restriction enzymes are abbreviated as follows: RI, *Eco*RI; Sc, *Sac*I; Sp, *Sph*I; H, *Hind*III; K, *Kpn*I; SI, *Sal*I. Genes with identical putative functions are depicted by identical shading. The gene names are as in previous reports.

fragment of *Hind*III–*Hind*III, including downstream of *hdcA*, and 2·3-kb fragment of *Eco*RI–*Sph*I, including upstream of *hdcT* (Fig. 1). Positive clones were selected by colony blot hybridization (Sambrook *et al.* 1989), and the obtained plasmids were designated as pSS45, pHH45 and pES23 (Table 1).

Plasmid DNA from *E. coli* strains was extracted by a commercially available kit and sequenced using a Dye Terminator Cycle Sequencing kit (Applied Biosystems, Foster City, CA, USA) on a 373A DNA Sequencer (Applied Biosystems). Sequence data were compiled and analysed using Genetyx-Mac genetic information processing software (Software Development, Tokyo, Japan). Possible transcriptional terminator, ribosome binding site and promoter elements were predicted by Genetyx-Mac. The BLAST program was used to identify sequences similar to the deduced amino acid sequences in the DNA Data Bank of Japan (DDBJ) (Altschul *et al.* 1997). The hydrophobicity and the possible transmembrane domains of *hdcT* gene products were calculated and plotted using the TMpred program (Hofmann and Stoffel 1993) and by the SOSUI program (Hirokawa *et al.* 1998). Multiple sequence alignment and calculation of the phylogenetic relationships were performed using CLUSTALW (Thompson *et al.* 1994) with exclusion of alignment gaps for analysing phylogenetic relationships.

Expression of *hdc* gene in *E. coli*

The *Sac*I–*Kpn*I fragment containing the *hdcA* gene was subcloned into the pUC18 and pUC19 plasmids to obtain pSK18 and pSK19 and transformed into *E. coli* BL21 (DE3) cells (Novagen, Madison, WI, USA). Recombinant *E. coli* BL21 (DE3) cells harbouring plasmids pSS45 (containing both of *hdcT* and *hdcA*), pSK18, and pSK19 were cultured in 5 ml of modified LB medium (LB broth containing 10 g l^{-1} L-histidine). After centrifugation at 15 000 *g* for 10 min, the supernatant was filtered through

Table 1 Strains and plasmids used in this study

Strain or plasmid	Relevant characteristics	Source or reference
Bacterial strains		
Photobacterium damselae		
ATCC 51805	Isolated strain from fish as a histamine producer	Okuzumi *et al.* (1981), Kimura *et al.* (2000)
Escherichia coli		
JM109	*recAI, endAI, gyrA96, thi, hsdR17(rK- mK+), Δ lac-proAB/F'[traD36,proAB+, lac I^q, lacZ Δ M15]*	Toyobo
BL21 (DE3)	F-, *lon*, *ompT*, *hsdS$_B$*($r_B^-m_B^-$), *dcm*, gal, (DE3)	Novagen
Plasmids		
pUC18	*lacZ*, Amp^r, Multiple cloning site	Takara bio
pUC19	*lacZ*, Amp^r, Multiple cloning site	Takara bio
pSS45	pUC18 plasmid vector containing 4.5 kb *SacI-SalI* fragment including *hdc A* and *hdc T*	This study
pES23	pUC18 plasmid vector containing 2.3 kb *EcoRI-SphI* fragment from *P. damselae* genomic DNA covering the upstream region *of hdc T*	This study
pHH45	pUC18 plasmid vector containing 2.3 kb *HindIII* fragment from *P. damselae* genomic DNA covering the downstream region *of hdc A*	This study
pSK18*	pUC18 plasmid vector containing *hdc A* gene together with 0.8 kb of the upstream region and 0.3 kb of the downstream region	This study
pSK19†	pUC19 plasmid vector containing *hdc A* gene together with 0.8 kb of the upstream region and 0.3 kb of the downstream region	This study

*The inserted fragment was placed in the opposite orientation from *lac* promoter of pUC18 plasmid.
†The inserted fragment was placed under the control of *lac* promoter originated from pUC19 plasmid.

0·22 μm filtre (Advantec Toyo, Tokyo, Japan) and the histamine content of the supernatant was analysed by reversed phase HPLC (Yamanaka and Matsumoto 1989).

RNA isolation and Northern hybridization

Aliquots (100 μl) of overnight *P. damselae* cultures in PY-7·5 were inoculated into 50 ml of PY-7·5 in 100ml culture flasks and incubated aerobically at 30°C in a reciprocal shaker set at 200 rev min^{-1}. When the cultures reached an optical density of around 0·1 at 550 nm, 10 ml aliquots were removed and centrifuged, and cells were resuspended in 10 ml of PY-4·5, PY-7·5, HB-4·5, or HB-7·5 which were prepared as described above, and incubated in screw cap tubes (20 × 125 mm) in a stationary incubator at 30°C for 3 h. Tubes were shaken gently every 30 min to prevent cells from settling. Cells from these cultures were harvested by centrifugation at 10 000 *g* for 5 min and total RNA was isolated using TRIzol reagent (Invitrogen, Carlsbad, CA, USA) by the acid guanidium isothiocyanate–phenol–chloroform method. Samples containing 20 μg of total RNA were electrophoresed on 1% agarose gel containing 6·6% formaldehyde along with a 0·2- to 10-kb RNA ladder (Novagen) for size determination. RNA was transferred to a positively charged nylon membrane (Hybond-N$^+$; Amersham Biosciences) and hybridized to labelled DNA probes. Hybridization was performed with AlkPhos Direct Nucleic acid labeling and detection system using DNA probes specific for *hdcA* or *hdcT*, prepared by PCR using primers 5′-ATG CTT TTT GGG CTC ACT GC-3′ and 5′-GAT GGT GAG CAG ATA CCA CC-3′ for *hdcA*, and 5′-TTT ATT GGA TTA GCG CAT GG-3′ and 5′-ACA GAT TTA CCA CTG TGT GC-3′ for *hdcT*.

RT-PCR for mRNA quantification

Primer selection

All reverse transcription reactions were carried out with randomly synthesized hexanucleotide [random hexamer, d(N)$_6$, Takara Bio]. A total of five primer sets were designed to study the transcription of *hdcT*, *hdcA* and *hisRS* gene of *P. damselae* with the following transcript sizes: *hdcT* (408 bp), 5′-CGG AAT TGT CGC TTA TGC CAA-3′ and 5′-CGC CTA AGA AAC CCC ACA ATG-3′, *hdcA* (273 bp), 5′-AAG AGC CAG GTT GTC GAG TCA-3′ and 5′-CGG CAT CGG CAT GGA TAT AA-3′; and *hisRS* (107 bp), 5′-TGA GGT ATG GCC TTT TCC ACT A-3′ and 5′-CTA CCC ATT GCC AAA TAG GTG T-3 '. The *hdcT-hdcA* bi-cistronic cDNA was detected by primers 5′-TTT TAA CTG CCA TTG GGA CGA-3′ and 5′-AGT GCG CCC AAA ATG CAT CTA-3′, which were designed

to target the C-termini of *hdcT* and the N-termini of *hdcA* with an amplicon length of 273 bp. The *hdcA-hisRS* bi-cistronic cDNA was detected by primers 5′-TGC TCA CCA TCT TAC ACA TGA A-3′ and 5′-AAG GCC ATA CCT CAT AGA GAG G-3′, which were designed to target the C-termini of *hdcA* and the N-termini of *hisRS* at an amplicon length of 126 bp. Universal primers 338f and 539r were used to amplify 16S rRNA for an endogenous control.

Reverse transcription of RNAs

RT reactions were carried out using the PrimeScript RT reagent kit (Takara Bio) with 200 ng of total RNA according to the manufacturer instructions.

Amplification

Real-time PCR was performed using the ABI 7900HT sequence-detection system (Applied Biosystems) with 25 μl reaction mixtures containing 12·5 μl of SYBR Premix Ex Taq (Takara Bio), 0·5 μl of ROX (6-carboxy-X-rhodamine, Takara Bio) reference dye, 0·4 μmol l^{-1} each primer, and 2 μl of template cDNA (or known concentrations of genomic DNA) solution with the following thermal protocol: 95°C for 15 s; 40 cycles of 95°C for 10 s and 60°C for 45 s; and an extension phase for dissociation analysis according to manufacturer instructions. All runs included standard templates for calculating a standard curve for amplification efficiency, as well as controls with no reverse transcription and no templates. After confirming amplification specificity by dissociation curve analysis, results were subjected to data analysis as described below. All reaction mixtures were electrophoresed on agarose gels followed by visualization by ethidium bromide staining.

Data analyses

The fluorescent signals were normalized against the reference dye (6-carboxy-X-rhodamine; ROX, included in the SYBR Green buffer) and were used to calculate the ΔRn using Rn^+ (normalized signal)–Rn^- (baseline Rn during cycles 3–15). Data were plotted as ΔRn against the PCR cycle number, with the threshold ΔRn set at 10 times the standard deviation of the mean baseline signal calculated for Rn^-. The threshold cycle (Ct) was defined as the cycle number at which ΔRn fluorescence crossed the threshold for a sample. The standard curve between Ct and the amount of DNA for each primer pair was drawn using 10-fold serial dilutions of genomic DNA and used to calculate the amount of mRNA in each sample. To correct for the total cell number in the RNA extraction and extraction efficiency, the quantity of 16S rRNA in each sample was used for the endogenous control, assuming that the expression of 16S rRNA is constant for all cells used in this mRNA expression analysis.

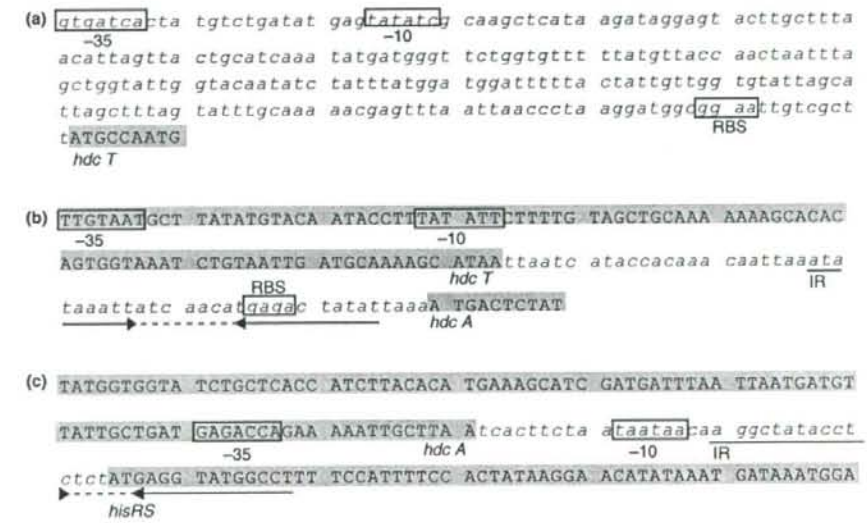

Figure 2 The abstracted representation of the upstream region of the *hdcT* gene (a), *hdcT-hdcA* intergenic region (b), and *hdcA-hisRS* intergenic region (c). Protein coding regions are shown in capital letters on grey background. Putative promoter elements and putative ribosomal binding sites (RBS) are indicated by boxes. The putative transcriptional terminator elements (inverted repeat, IR) are indicated by solid arrows (stems) and dashed lines (loops).

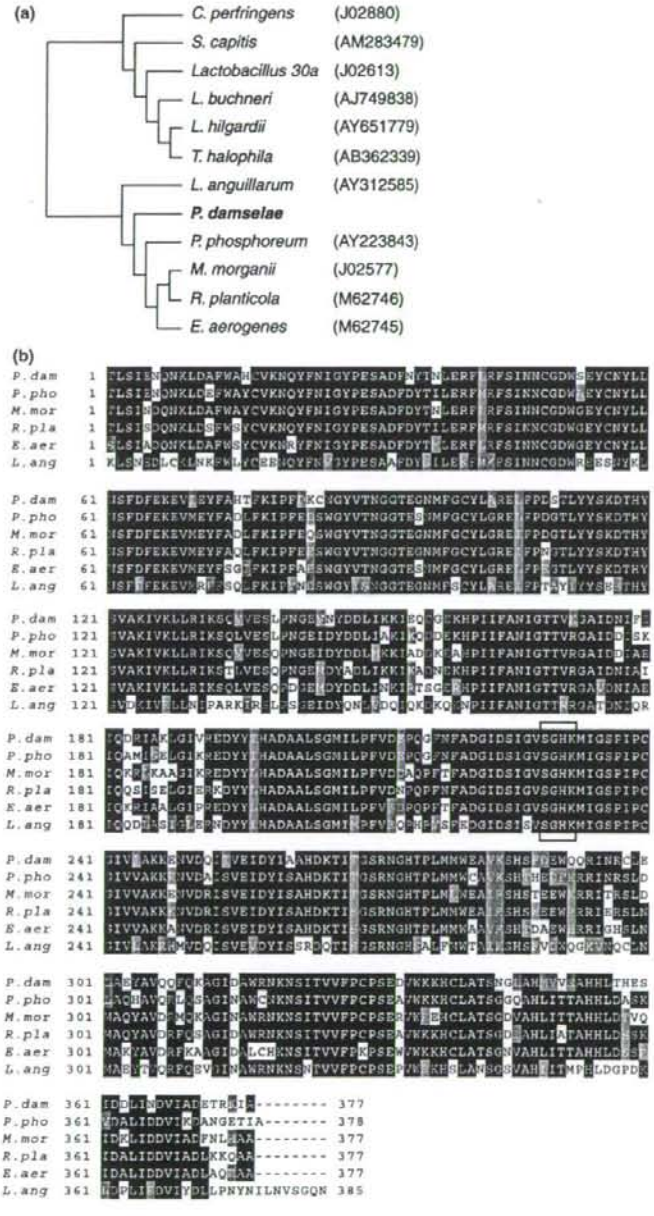

Figure 3 (a) Phylogenetic relationships of bacteria based on deduced HdcA amino acid sequences. Distances between sequences were calculated by CLUSTALW software (excluding the alignment gaps) and dendrograms were drawn by the neighbour-joining method. The nucleotide sequence accession numbers are shown in parenthesis. (b) Amino acid sequence alignment of HdcA in the following bacteria: P. dam, *Photobacterium damselae*; P. pho, *P. phosphoreum*; M. mor, *Morganella morganii*; R. pla, *Raoultella planticola*; E. aer, *Enterobacter aerogenes*; and L. ang, *L. anguillarum*. Identical residues (white letters on black background) and similar residues (white letters on grey background) are indicated.

Nucleotide sequence accession number

The 6083-bp nucleotide sequence of *P. damselae hdc* gene cluster determined in this study has been submitted to the DDBJ database under accession no. AB363972.

Results

Isolation and sequencing of the *hdc* and related genes of *P. damselae*

Amino acid sequencing of the subunits of the purified histidine decarboxylase of *P. damselae* (TLSIENQNKLDAFWAHCVKNQYFNI) revealed the N-terminal sequence to be highly similar to previously reported histidine decarboxylase sequences of *M. morganii*, *R. planticola* and *E. aerogenes* (Vaaler *et al.* 1986; Kamath *et al.* 1991). Cloning the 4·5kb *Sac*I–*Sal*I fragment after Southern blot hybridization analysis first revealed *hdcT*, *hdcA* and incomplete ORFs (Fig. 1); therefore, two adjacent fragments were cloned. In total, we sequenced 6083 bp around the *hdcA* gene and found three open reading frame (ORF) sequences and one 3′ partial ORF (>1311 bp) on the same strand. We designated these three ORFs as *hdcT*, *hdcA* and *hisRS*, respectively (Fig. 1). A 3′ partial ORF found at 808-bp upstream of *hdcT* was designated as *orf4*.

Sequence analysis of the *hdc* cluster from *P. damselae*

hdcA

The putative histidine decarboxylase gene, designated as *hdcA* in *P. damselae*, is 1131 bp in length with an initial start codon (ATG) and a stop codon (TAA) at the 3′-end followed by a 12-base inverted repeat, which represents a potential transcription termination site (Fig. 2c). A putative ribosome binding site sequence (dGAGA) is located 10-bp upstream of the translational start codon for *hdcA* (Fig. 2b). The G + C content of the gene was 44% and the molecular weight of the encoded polypeptide of 42 833 Da compares well with earlier reports for subunits of this enzyme from other known *Enterobacteriaceae* (Kamath *et al.* 1991).

The deduced amino acid sequence of *P. damselae* HdcA shares significant sequence similarity with those of *P. phosphoreum*, *M. morganii*, *R. planticola*, *E. aerogenes* and *L. anguillarum* (Fig. 3b). Each enzyme contains 377 or 378 amino acid residues with an overall high sequence similarity of 80%; the lowest similarity is observed in regions between residues 141 and 193 and residues 279–319 (Fig. 3b). Comparison with known decarboxylases revealed that the important catalytic residue lysine at position 234 (K234), with which that pyridoxal 5′-phosphate forms an internal aldimine (Schiff base linkage), was found in HdcA of *P. damselae*. The residues around K234, Ser-Gly-His were conserved in PLP-dependent histidine decarboxylases (Vaaler *et al.* 1986; Kamath *et al.* 1991) (Fig. 3b).

hdcT

This 1143-bp ORF positioned at 43-bp upstream of *hdcA* initiation codon shows the most significant similarity to HdcT compared to membrane proteins, putative amino acid permease of *Salmonella* Paratyphi A and putrescine/ornithine antiporter of *Salmonella* chorelaesuis based on BLAST program search (58% similarity and 38% identity, based on deduced amino acid sequence).

To understand the physiological role of *hdcT*, the hydrophobicity profile of HdcT and other well characterized amino acid/amine antiporters (HdcC of *Lactobacillus buchneri*, HdcP of *Staphylococcus capitis*, and PotE and CadB of *E. coli*) were determined (Fig. 4a). Although the numbers of hydrophobic domains differed between these five proteins, HdcT showed hydrophobic patterns similar to those of the other membrane proteins. The total number of transmembrane spans in the predicted structure of *P. damselae* HdcT is 10 or 11, depending on whether the Serine residue at position 345 was regarded as a transmembrane domain or not, and similar transmembrane regions were observed at the second to sixth transmembrane domains based on comparisons with other amino acid/amine antiporter proteins (Fig. 4b).

hisRS

The deduced amino acid sequence of *hisRS*, located 33 bp downstream of the stop codon of *hdcA* gene, showed significant similarity to histidyl-tRNA synthetase of several bacteria, such as *Haemophilus* sp., *Yersinia* sp. and *Vibrio* sp., ranging from 71% to 68% (data not shown).

Amino acid sequence comparison between HisRS of *P. damselae* and histidyl-tRNA synthetase of *E. coli* (Arnez *et al.* 1995; Guth and Francklyn 2007) identified three conserved motifs of class II aminoacyl-tRNA synthetase (Fig. 5, motifs 1–3). The residues R127, Q129 and R132 were reported to enforce the specificity of histidyl-tRNA synthetase for histidyl-tRNA of *E. coli* (Guth and Francklyn 2007). The conserved residues at positions 268–276, indicated by solid stars in Fig. 5, comprising one wall of the histidine binding pocket in *E. coli* (Arnez *et al.* 1995). According to Arnez *et al.* (1995), the conserved domain at positions 296–303 comprises the floor and back pocket of histidine substrate.

orf4

The closest matches produced by the BLAST search for the deduced amino acid sequence of the 3′ partial ORF

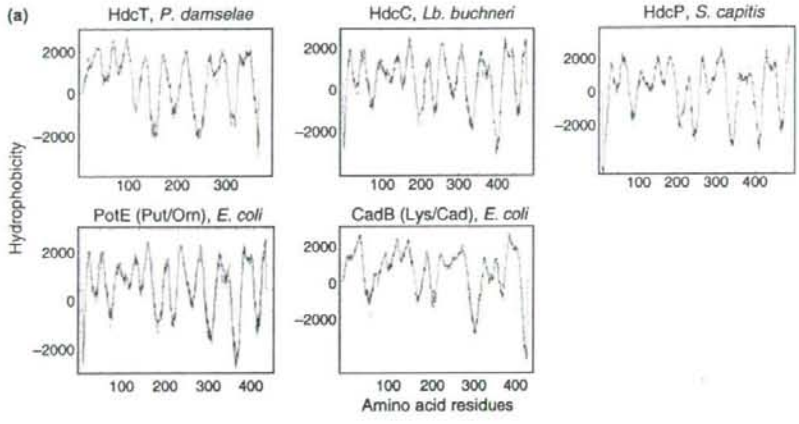

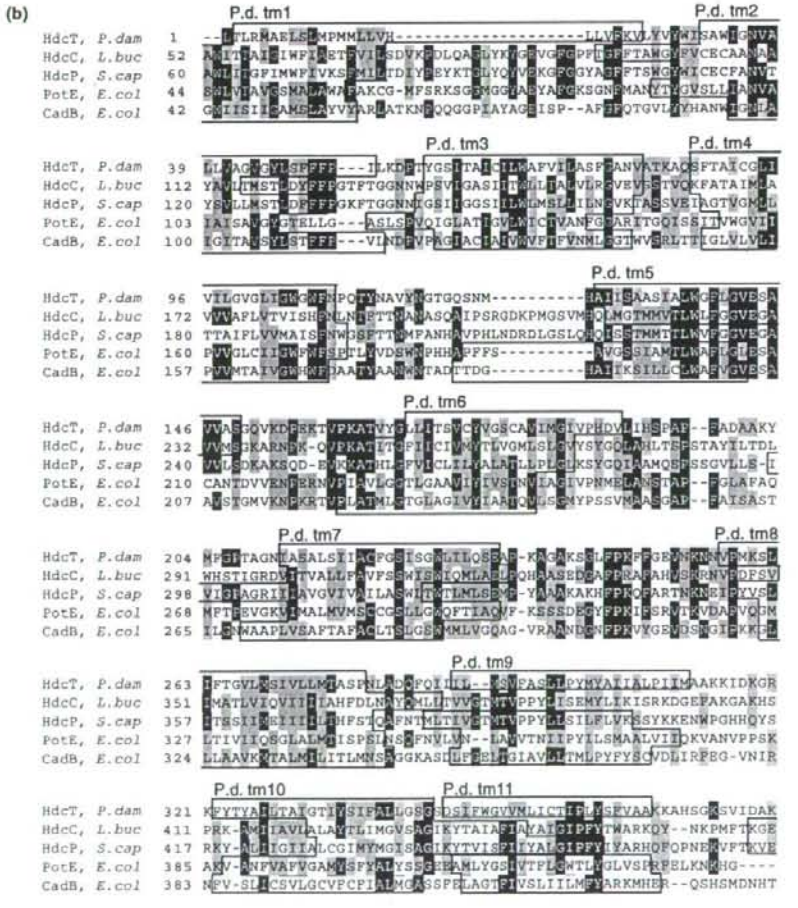

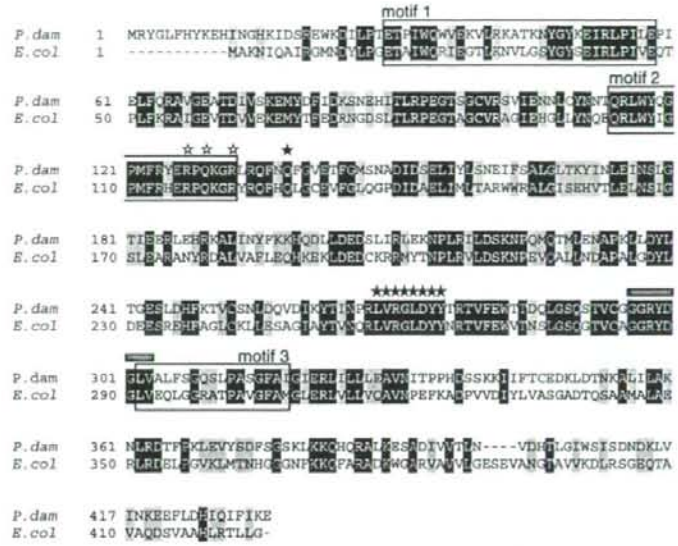

Figure 5 Alignment of the deduced amino acid sequence for *hisRS* of *Photobacterium damselae* and histydyl-tRNA synthetase of *Escherichia coli*. The identical (white letters on black background) and similar (white letters on grey background) amino acid residues are indicated. The significantly conserved domains of class II aminoacyl-tRNA synthetase protein are boxed (motifs 1–3). Open stars indicate important residues for specificity of histidyl-tRNA synthetase to histidyl-tRNA molecules in *E. coli* (Guth and Francklyn 2007). Closed stars and grey bar indicate domains related to the interaction of histidine substrate with histidyl-tRNA synthetase in *E. coli* (Arnez *et al.* 1995).

(>1311 bp) found 808 bp upstream of the *hdcT* start codon were putative helicases from various sources, such as *Shewanella oneidensis* (76% similarity, AE014299) and *Vibrio chorelae* (75% similarity, EDL74353).

Expression of *hdc* gene in *E. coli*

To confirm the function of the *hdcA* gene, histamine excretion was measured in cultures of *E. coli* cells harbouring plasmids pSS45 (containing *hdcT* and *hdcA*), pSK18 and pSK19. Plasmids pSK19 and pSK18 contained only the complete *hdcA* ORF under control of the *lac* promoter and in the opposite orientation to the *lac* promoter, respectively (Table 1). After 5 h of incubation, the transformants harbouring pSK18 and pSK19 produced histamine at 18·4 ppm and 26·6 ppm, respectively. The transformant harbouring pSS45 produced histamine at a concentration of 916 ppm (Fig. 6). In cultures of *E. coli* BL21 (DE3) harbouring the pUC 18 vector alone, no histamine was detected.

Transcriptional analysis of *hdc* operon

Northern blot with labelled *hdcA* gene fragments showed a major *hdcA*-hybridizing band corresponding to the 1·25-kb transcript, at both pH 4·5 and 7·5 (Fig. 7a). The size corresponds to the predicted size for the *hdcA* monocistronic transcript. Another hybridizing band, with a size of 2·5 kb, was detected from cells cultured with histidine at pH 4·5 or pH 7·5 (Fig. 7a). The fragment sizes corresponded to those predicted for *hdcT-hdcA* or *hdcA-hisRS* co-transcripts. Similar expression patterns were observed for the use of partial DNA of *hdcT* as a probe; a 1·25 kb band for *hdcT* monocistronic transcript and the 2·5 kb

Figure 4 Comparison of the HdcT and other amino acid/amine antiporters. (a) Hydrophobicity plots calculated using TMpred. (b) Multiple sequence alignment of the deduced amino acid sequences. Amino acid residues identical (white letters on black background) and similar (white letters on grey background) for more than three sequences per site are indicated. Predicted transmembrane domains of HdcT of *Photobacterium damselae*, HdcC of *Lactobacillus buchneri* (AJ749838) and HdcP of *S. capitis* (AM283479) using SOSUI program, and that of previously reported PotE (putrescine/ornithine antiporter, Kashiwagi *et al.* 1999) and CadB (lysine/cadaverine antiporter, Soksawamakhin *et al.* 2005) of *Escherichia coli* are indicated by boxes.

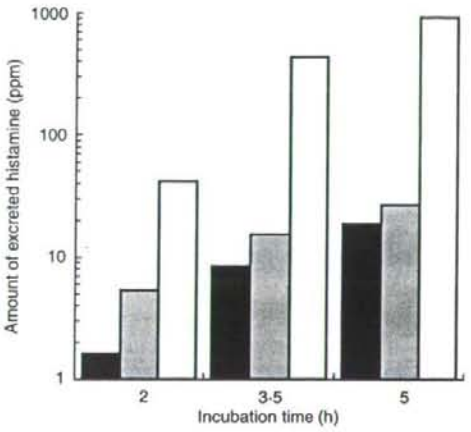

Figure 6 Expression of *hdcA* or *hdcT-hdcA* genes of *Photobacterium damselae* in *Escherichia coli* BL21 (DE3). Fragments containing only *hdcA* or both *hdcA* and *hdcB* were subcloned into pUC18/19 plasmid vectors followed by transformation into *E. coli* BL21 (DE3) to obtain pSK18-DE3 (solid bars, containing *hdcA* gene in the opposite orientation to the *lac* promoter), pSK19-DE3 (grey bars, containing *hdcA* gene under control of the *lac* promoter) and pSS45-DE3 (open bars, containing both *hdcA* and *hdcB* genes under control of the *lac* promoter). Transformants were cultured in LB medium containing 1% l-histidine and 1 mmol l^{-1} IPTG, and culture supernatants were then collected and the concentration of histamine was measured. In cultures of *E. coli* BL21 (DE3) harbouring only the pUC 18 vector, no histamine was detected.

band correspond to *hdcT-hdcA* transcript were detected as a major band at pH 4·5 (Fig. 7a). Under the incubation condition of pH 4·5 with histidine, the 4·0 kb transcript, corresponded to the *hdcT-hdcA-hisRS* tri-cistronic transcript was observed with both of *hdcT* and *hdcA* probes (Fig. 7a). To summarize, six types of transcripts were detected from *P. damselae hdc* gene cluster: *hdcT*, *hdcA*, *hisRS*, *hdcT-hdcA*, *hdcA-hisRS* and *hdcT-hdcA-hisRS*. Transcript number was higher at pH 4·5 than pH 7·5, and under histidine excess (Fig. 7a).

To precisely compare the expression ratio among these conditions, quantitative RT-PCR was performed. The most abundant transcripts of each genes were detected at pH 4·5 with histidine excess (Fig. 7b, hatched bars). The expression of each gene was reduced 10^{-1} to 50^{-1} fold both at pH 4·5 without histidine and at pH 7·5 with histidine excess (Fig. 7b). However, the transcript amount under these conditions was not significantly different, except for *hdcA*, which was slightly higher than the other four ($P < 0{\cdot}05$). On the other hand, at pH 7·5 without addition of histidine, all of these genes showed significantly less transcription than under the other conditions. At pH 7·5 without addition of histidine, *hisRS* mRNA was most abundant with *hdcT* and *hdcA* at 0·73 and 0·38 log difference, respectively.

Discussion

We isolated and sequenced the histidine decarboxylase gene (*hdcA*), which showed high identity with the amino acid sequences of histidine decarboxylases of other known Gram-negative bacteria: *M. morganii* (79·6% identity), *R. planticola* (79·1%), and *E. aerogenes* (76·9%) (Vaaler *et al.* 1986; Kamath *et al.* 1991); *P. phosphoreum* (80·2%, Morii *et al.* 2006); and *P. damselae* (100%, Kanki *et al.* 2007) (Fig. 3). The deduced amino acid sequence of HdcA was comprised of the determined N-terminal amino acid sequence with the exception of a methionine at the first residue. The first methionine was presumed to be removed at maturation, as has previously been shown for other HdcA of *R. planticola* and *E. aerogenes* (Guirard and Snell 1987; Kamath *et al.* 1991). These pyridoxalphosphate dependent histidine decarboxylase genes, which are distributed among Gram-negative bacteria, are thought to have evolved from a common ancestral gene (Fig. 3a).

To confirm the function of the *hdcT* and *hdcA* genes of *P. damselae*, *hdcA or hdcT-hdcA* genes were expressed in *E. coli*. Plasmids containing the *hdcA* gene enabled the transformed *E. coli* strain to produce histamine (Fig. 6); therefore, we concluded that *hdcA* encodes histidine decarboxylase. Histamine concentration in cultures of recombinants harbouring pSS45 was almost 50 times greater than in cultures of recombinants harbouring pSK19 in IPTG-induced conditions, indicating that *hdcT*, an upstream genetic element of *hdcA* has a positive effect for either *hdcA* expression level or the excretion level of histamine. The hydrophobicity of the amino acid sequence of HdcT (Fig. 3a) suggests that HdcB is located in the cytoplasmic membrane. The sequence alignment and comparison of predicted transmembrane domains between well characterized amino acid/amine antiporters, PotE (Kashiwagi *et al.* 2000) and CadB (Soksawatmaekhin *et al.* 2006) (Fig. 3b) support this finding. Moreover, comparison of HdcT between other amino acid/amine antiporters revealed several conserved residues of histidine/histamine antiporter proteins from Gram-positive bacteria. Therefore, HdcT is strongly suggested to be a histidine/histamine antiporter in *P. damselae*. This is consisted with the observation of larger amounts of histamine in cultures of *E. coli* harbouring pSS45 (containing both of *hdcT* and *hdcA*) than in cultures of *E. coli* harbouring pSK18/19 (containing *hdcA*).

Northern blot experiments and quantitative RT-PCR revealed the *hdc* genes were highly induced under acidic

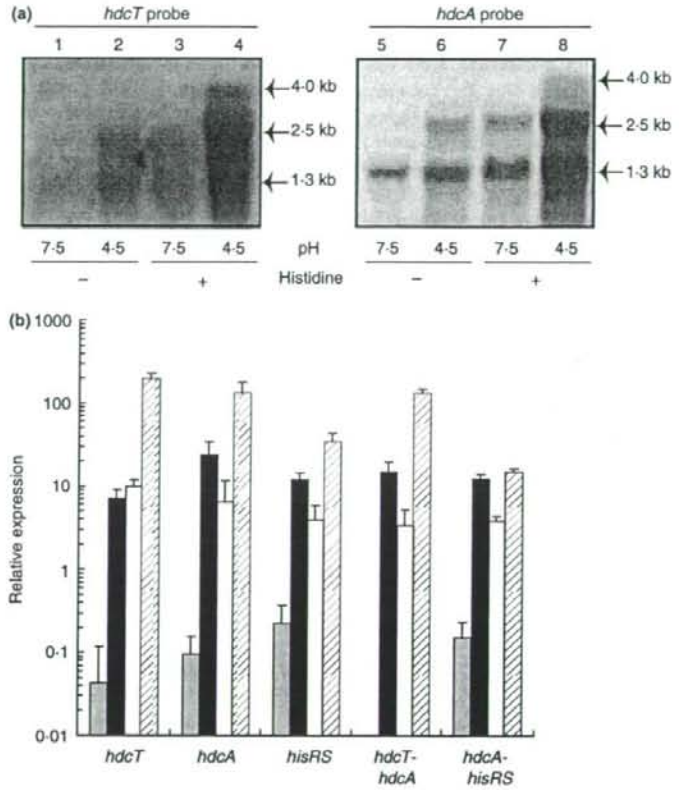

Figure 7 Transcriptional analyses of the *hdc* genes of *P. damselae* under different culture conditions. (a) Northern blot hybridization. Lanes 1 and 5, pH 7·5; lane 2 and 6, pH 4·5; lane 3 and 7, pH 7·5 with histidine; lane 4 and 8, pH 4·5 with histidine. Aliquots (20 μg) of total RNA were electrophoresed and blotted to membranes followed by hybridization with *hdcT* (lanes 1–4) or *hdcA* (lanes 5–8) probes. (b) Quantification of mRNA extracted from cells treated with pH 7·5 (grey bars), pH 4·5 (solid bars), pH 7·5 with histidine (white bars), and pH 4·5 with histidine (hatched bars). cDNA was quantified against a standard curve produced using genomic DNA. The relative amount of 1 is approx. equal to 10^3 copies of genomic DNA per reaction. Bars represent the averages of three experiments, and error bars indicate the SD.

conditions or histidine-rich condition, or both. Both mono- and poly-cistronic transcription were observed. The intense band corresponding to a 2·5-kb transcript at pH 4·5 in the presence of histidine, as revealed by both *hdcA* and *hdcT* probes, indicates that the *hdcTA* co-transcript is a major transcriptional product under this condition and these were also evidenced by RT-PCR. On the other hand, *hdcTA* transcription was not detected under pH 7·5 without histidine condition (Fig. 7b), while both mono-cistronic *hdcT* and *hdcA* mRNA were detected. This is consistent with previous reports of *cadBA* operon of *V. cholerae* (Merrell and Camilli 2000). However, the reason for transcription of these *hdc* genes as either bi- or mono-cistronic messages remains to be elucidated. Morii and Kasama (1995, 2004) and Morii *et al.* (2006) reported that the decarboxylation of histidine by *P. phosphoreum* was achieved by two types of histidine decarboxylase enzymes (constitutive and inducible), which could be separated and fractionated by gel chromatography. However, our Southern hybridization results using different enzyme combinations showed that a single *hdc* gene was present on the chromosome of *P. damselae* (data not shown). The presence of *hdcT* and *hdcA* monocistronic transcripts at an amount almost 100-fold greater than under acidic or histidine excess condition (Fig. 7b) indicates that the *hdcA* gene was expressed constitutively in *P. damselae* although at lower amounts than under low pH or histidine excess conditions.

It is interesting that the *hisRS* gene, the putative histidyl-tRNA synthetase gene, was found immediately downstream